



Optimization of Roof Coverage and Tank Size for Integrated Green Roof Rainwater Harvesting Systems—a Case Study

Haowen Xie¹ · Mark Randall² · Sylvana Melo dos Santos³

Received: 16 August 2022 / Accepted: 24 July 2023 / Published online: 14 September 2023
© The Author(s), under exclusive licence to Springer Nature B.V. 2023

Abstract

Rainwater harvesting (RWH) systems are effective in alleviating water supply shortages, while green roofs (GRs) can contribute to stormwater management, air quality improvement, thermal regulation of buildings, and biodiversity support. Despite their individual benefits, both systems are not frequently combined. This paper investigates the potential for integrating these systems through a hydrologic modeling and optimization approach, using a case study in Paris, France. The study utilized a Conceptual Interflow model (CI-model) coupled with a Water Balance (WB) model to describe the rainfall-runoff relationship of integrated green roof and rainwater harvesting (GR-RWH) systems. An NSGA-II optimization was then applied to the CI-WB model to determine the optimal tank sizing of GR-RWH systems for meeting different water demands. The results show that GR-RWH systems have water reliability (WR) values similar to those of traditional RWH systems without GR, albeit with larger tank volumes. For new buildings in Paris, a GR-RWH system with approximately 25 to 75% GR coverage meets rainwater utilization needs with low investment while also providing the added benefits of GRs.

Keywords Green roof · Runoff modelling · Optimization analysis · Economic feasibility · Rainwater harvesting · Return on investment period

1 Introduction

Water security is a critical global issue that requires attention (UN 2015). Rainwater harvesting (RWH) is a sustainable strategy that involves the collection and storage of rainwater for various purposes, including domestic, commercial, and industrial use (Campisano et al. 2017; Dallman et al. 2017; Imteaz et al. 2012; Souto et al. 2023; Yang et al. 2023).

Highlights

- GR-RWH systems require a slightly larger tank volume than RWH to achieve similar water reliability under the same water demand.
- For new building design in Paris, a GR-RWH system with 25 to 75% GR coverage is a promising option due to its cost-effectiveness in meeting rainwater utilization needs while providing additional GR benefits.
- Existing buildings in Paris with a GR could potentially benefit economically from the addition of RWH.

Extended author information available on the last page of the article

Table 1 Summary of studies of GR and RWH used in combination

Location	Water use	Method to calculate rooftop runoff	Reference
Georgia (US)	Irrigation	No mention	Lynch and Dietsch (2010)
Florida (US)	Irrigation	RCM	Hardin et al. (2012)
Brazil	Irrigation	RCM	Vieira et al. (2013)
Taiwan (China)	Irrigation	RCM	Chao-Hsien et al. (2015)
Hong Kong (China)	Irrigation Toilet flushing	RCM	An et al. (2015)
Greece	Irrigation Toilet flushing	RCM	Monteiro et al. (2016)
S. Miguel Island Azores(Portugal)	Non-potable use	RCM	Santos and Taveira-Pinto (2013)
Brazil	Potable use	RCM	Santos et al. (2019)
Portugal	Non-potable use	RCM	Almeida et al. (2021)

Although rainwater harvesting (RWH) can contribute to the provision of water supply, it is insufficient in addressing a range of urban issues resulting from rapid socio-economic changes, population growth, urbanization, and climate change. These challenges include urban heat island, air pollution, urban noise, and energy shortages. (Campisano et al. 2017; Cook and Larsen 2021; Mitchell et al. 2008; Sampson et al. 2020). This study investigates whether the integration of green roofs (GRs) with RWH could be an effective solution to address multiple urban issues in a synergistic manner.

GRs offer several benefits, such as supporting biodiversity, prolonging the lifespan of hard roofs, reducing stormwater runoff and mitigating combined sewer overflow, improving building insulation, and moderating air temperatures. However, the extent of these effects is influenced by the local context and design specifics (Berardi et al. 2014; Francis and Jensen 2017; Kolokotsa et al. 2013; Lepp 2008; Oberndorfer et al. 2007; Quaranta et al. 2021; Sadeghi et al. 2019; Singh et al. 2020). Moreover, the water discharged from GRs has been found to be appropriate for non-potable applications, such as landscape irrigation and toilet flushing. (Razzaghmanesh et al. 2014; Van Mechelen et al. 2015).

Table 1 presents the studies that have investigated the integration of GRs with RWH. The Runoff Coefficient Method (RCM) was utilized in these studies to estimate runoff by multiplying the appropriate Runoff Coefficient by rainfall (Abdulla 2020; Alim et al. 2020; Maykot and Ghisi 2020).

At the public building scale (i.e. area = 8400 m²), C. Santos and Taveira-Pinto (2013) conducted an analysis of a building with an estimated occupancy of 740 individuals. The design team considered the supply of rainwater to toilets and urinals by collecting runoff from the GR area in an underground tank. The study found that the payback period for this system, i.e., the time it takes for the investment to be recovered, ranged between 17 to 23 years. Hardin et al. (2012) reported that the installation of a rainwater tank on a green roof led to an increase in the total annual stormwater retention on the study site from 43 to 87% in Florida.

In Santos et al. (2019), the potential benefits of using GRs for both building insulation and RWH were investigated in a semi-arid region by observing temperature reductions in rooms located under a green cactus roof. The study found that the installation of GRs over bedrooms could significantly lower the room temperature while only causing a minor

reduction (18%) in total annual runoff volume. In another study by Almeida et al. (2021), a comparison was made between a flat traditional roof and one incorporating an extensive GR with RWH. The study found that the GR-RWH combined solution resulted in a potential water saving decrease of less than 6% while increasing the volume of retained water by almost 15% compared to RWH alone.

While several publications have investigated the water supply aspects of GR-RWH systems (as shown in Table 1), studies that focus solely on RWH are more prevalent (Alim et al. 2020; Maykot and Ghisi 2020; Oberascher et al. 2019; Palermo et al. 2019; Słyś and Stec 2020; Stec and Zeleňáková 2019; Tamane et al. 2021). To the best of the authors' knowledge, no comparative study has been conducted on the water supply of GR-RWH systems and conventional RWH systems, and how varying GR coverage ratios (R_{GR}) impact water supply under different roof areas. To address this research gap, the present study aims to employ mathematical models to compare the water supply performance of GR-RWH systems with different R_{GR} , and to identify the optimal R_{GR} for GR-RWH systems. The results of the study will provide valuable insights into the optimal design and operation of GR-RWH systems. The findings will be useful for policymakers, urban planners, and building designers in considering a variety of sustainable water management practices in urban areas.

This study presents a water balance model that aims to characterize the hydrological processes of green roof rainwater harvesting (GR-RWH) systems. Specifically, five different green roof ratios (R_{GR}) ranging from 0 to 100% are evaluated. To evaluate the economic viability and water reliability of GR-RWH, the water balance model is combined with an optimization method that employs the Non-dominated Sorting Genetic Algorithm II (NSGA-II).

The main objectives of this study are to answer three key questions:

- (i) How does the optimal tank size (V_t) vary based on different roof areas (RA), water demands (V_d), and R_{GR} (0, 25, 50, 75, and 100%)?
- (ii) Are GR-RWH systems with different R_{GR} economically feasible in terms of return on investment period and water reliability?
- (iii) What are the differences in return on investment period and water reliability of GR-RWH systems in water supply under varying RA, V_d , and R_{GR} ?

2 Methods

2.1 Hydrological Processes of Green Roof Rainwater-Harvesting Systems

Figure 1 depicts a schematic representation of the simulated GR-RWH system. To quantitatively characterize the hydrological dynamics of GR-RWH systems, we constructed a water balance model (WB-model) based on established techniques by previous authors (Dixon et al. 1999; Fewkes 2000; Słyś 2009). The equation for the WB-model of the GR-RWH system is presented in Eq. (1), where,

$$V_r + V_s = V_o + V_d \quad (1)$$

V_r is volume of roof runoff (m^3), which is less than or equal to the volume of the storage tank (V_t);

V_s is volume of tap water supplied to the system (m^3);

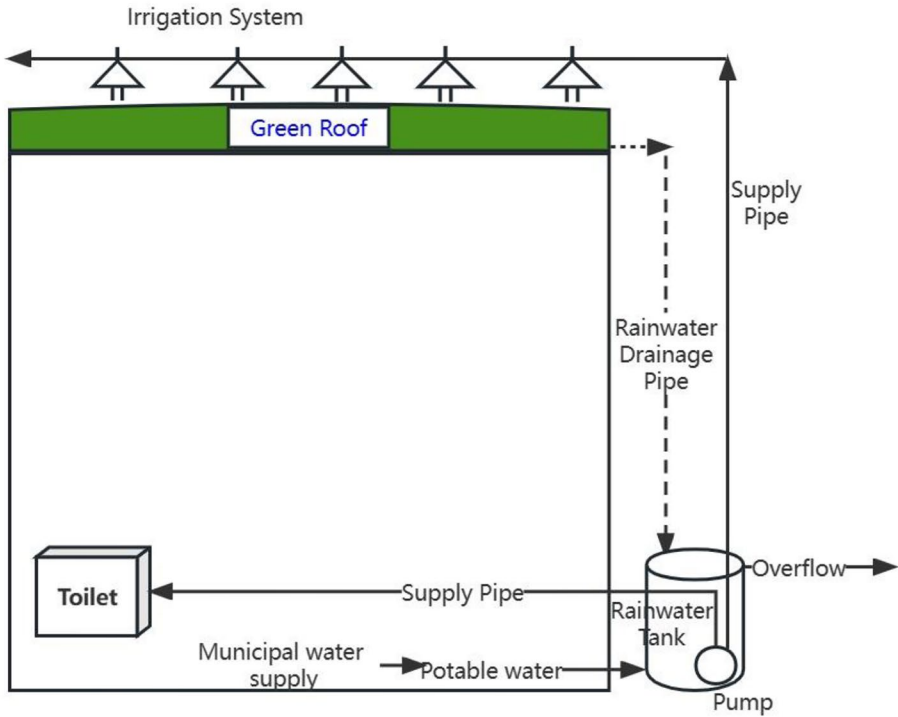


Fig. 1 Cross-section schematic of a building with GR-RWH system

V_o is volume of rainwater overflow to sewage system (m^3);
 V_d is water demand for non potable use (m^3/day).

In this study, a Conceptual Interflow model (CI-model) was used to assess the roof runoff from GR, as detailed in the Supplementary material (Eqs. S1–S7) (Xie and Liu 2020). Between rainfall events, moisture exits the system through the soil surface and vegetation via evaporation and transpiration. To estimate evapotranspiration (ET), we applied the modified Blaney-Criddle method (Eqs. 2 and 3), which has been previously used in related studies (Cascone et al. 2019; Cirkel et al. 2018; Jahanfar et al. 2018). During rainfall, we assumed that ET is negligible, following the findings of previous research (Carbone et al. 2014; Li and Babcock 2014; Zaremba et al. 2016).

$$PET = p(0.46T_{mean} + 8) \tag{2}$$

$$ET = \alpha \times PET \tag{3}$$

where PET is the potential ET, T_{mean} is mean daily temperature ($^{\circ}C$); p is mean daily percentage of annual daytime hours that is based on the latitude and month. α is a coefficient related to the antecedent precipitation index.

Several assumptions were made in the development of the model.

- (i) The largest volume of rainwater accumulated in the storage tank (V_r) was assumed to be equal to the capacity of the storage tank (V_t), with the volume of pump and pipes ignored.

- (ii) The demand for non-potable water in the house was assumed to be satisfied first by water accumulated in the storage tank, and only after by water from the conventional water-supply system.
- (iii) Any roof runoff in excess of the storage tank’s capacity (V_t) was assumed to be drained to the sewage system or to other rainwater-using equipment.
- (iv) The storage tank’s capacity was assumed to be more than the daily demand for non-potable water ($V_t > V_d$).
- (v) Snow buildup or sublimation were not taken into consideration in the model, therefore all precipitation was presumed to be rain.

The process of roof runoff filling and accumulation in the tank is described as follows:

$$\text{if } Vw_i + Vr_{i+1} > Vt, \text{ then } Vk_{i+1} = Vt \tag{4}$$

$$\text{if } Vw_i + Vr_{i+1} \leq Vt, \text{ then } Vk_{i+1} = Vw_i + Vp_{i+1} \tag{5}$$

The non-potable distribution system’s rainwater consumption from the storage tank is characterized by the following two conditions:

$$\text{if } Va_i - Vd_i < 0, \text{ then } Vw_i = 0 \text{ and } Vu_i = Va_i \tag{6}$$

$$\text{if } Va_i - Vd_i \geq 0, \text{ then } Vw_i = Va_i - Vd_i \text{ and } Vu_i = Vd_i \tag{7}$$

The tap water input to the non-potable distribution system is described as follows:

$$\text{if } Va_i > Vd_i, \text{ then } Vs_i = 0 \tag{8}$$

$$\text{if } Va_i \leq Vd_i, \text{ then } Vs_i = Vd_i - Va_i \tag{9}$$

The process of rainwater outflow (discharge) from the storage tank to the sewage system is defined as follows:

$$\text{if } Va_i + Vr_i \leq Vt, \text{ then } Vo_i = 0 \tag{10}$$

$$\text{if } Va_i + Vr_i > Vt, \text{ then } Vo_i = Vw_i + Vr_i - Vt \tag{11}$$

where:

The subscript i is the value at the i^{th} time interval, $i = 1, 2, \dots, n$. For instance, Va_i is the volume of rainwater held in the tank prior to the system drawing the water (consumption) at the i^{th} time interval (m^3); Vd_i is total water demand in the i^{th} time interval (m^3); Vk_i is the quantity of rainwater that remains in the tank at the conclusion of the i^{th} interval (m^3).

Vw is water volume in storage tank (m^3), which is less than or equal to Vr and maximum is Vt ;

Vu is volume of rainwater transferred from the storage tank to the distribution system (m^3).

2.1.1 Input Data for Conceptual Interflow Model

Versini et al. (2020) presented a comprehensive open data set derived from the Blue Green Wave (BGW), the largest Green Roof (1 hectare) in the Greater Paris Area. The BGW features a base depth of 20 cm and is predominantly covered with grasses, together with a mixture of perennial plants, grasses, and iris bulbs. A 300 mm diameter pipe collects water

from a wide area of the BGW (1143m²), referred to as the 'pipe drained region', with a depth sensor installed in the pipe to measure the flow rate (Q).

In the period spanning from February to May 2018, Versini et al. (2020) identified a total of six distinct rainfall events, each characterized by a cumulative rainfall depth exceeding 5 mm and separated by a dry interval of at least 6 h. Specifically, the identified events and their corresponding rainfall totals were as follows: R1 on March 7 (9 mm), R2 on March 11 (9.7 mm), R3 on March 17 (7.5 mm), R4 on March 27 and 28 (13.9 mm), R5 on April 9 (9.6 mm), and R6 on April 29 and 30 (23.5 mm). In this paper the events identified by Versini et al. (2020) were used; events R1-R3 to calibrate the CI-model, and events R4-R6 for validation.

2.1.2 Calibration and Validation

The overall runoff ratio (R_V) and Nash–Sutcliffe efficiency (NSE) were used in calibration and validation process. R_V is the ratio of simulated total runoff to observed total runoff. NSE has a range of $-\infty$ to 1, where a score of 1 indicates that the model is a perfect match, and a value of less than 0 indicates that the observed mean is a better predictor than the model (Nash and Sutcliffe 1970).

$$R_V = \frac{\sum_{t=1}^{t=t_f} Q_{sim}(t)\Delta t}{\sum_{t=1}^{t=t_f} Q_{mea}(t)\Delta t} \tag{12}$$

$$NSE = 1 - \frac{\sum_{t=1}^{t=t_f} (Q_{mea}(t) - Q_{sim}(t))^2}{\sum_{t=1}^{t=t_f} (Q_{mea}(t) - Q_{Amea})^2} \tag{13}$$

where: $Q_{sim}(t)$ =simulated flowrate; $Q_{mea}(t)$ =measured flowrate; Δt =time step; Q_{Amea} = average measured flowrate of individual events.

2.2 Optimization Model

The NSGA-II algorithm (Deb et al. 2002) is widely recognized as a prominent evolutionary multi-objective optimization (EMO) technique that aims to identify multiple Pareto-optimal solutions for a given multi-objective optimization problem.

The NSGA-II model was employed to identify the optimal volume of rainwater tank (Vt), using the optimization criteria $P_{ROI}(F1)$ and $WR(F2)$, which have been previously utilized in similar studies (Melville-Shreeve et al. 2016; Okoye et al. 2015):

$$F1 = \text{Minimize } P_{ROI} = \frac{I}{Be} \tag{14}$$

$$F2 = \text{Maximum } WR = \frac{X * 100\%}{365} \tag{15}$$

The NSGA-II optimization algorithm aims to minimize the objective functions, therefore, the Eq. (15) can be expressed as follows:

$$F2 = \text{Minimize } WUR = 1 - WR \tag{16}$$

where:

I is the total capital costs (euro),

Be is the benefit (euro/year), $Be = EV_d C$,

E is the tap water saving in the analyzed period (%),

C is the cost of tap water purchase (euro/m³), $C = 3.70(\text{€}/\text{m}^3)$ (l'eau 2015),

Water Reliability (WR) is the percentage of time that a household can depend on rainwater collected from their roof to fulfill their water requirements for one year (%),

Water Unsuitability Ratio (WUR) is the percentage of time that households cannot rely solely on rainwater and must supplement with other sources of water for one year (%),

X is the number of days per year where rainwater is sufficient to fulfill all household water needs.

The total capital costs I of the GR-RWH system consists of two parts: the capital costs of RWH (I_{RWH}) and the capital costs of GR (I_{GR}):

$$I = I_{RWH} + I_{GR} \tag{17}$$

For I_{RWH} (€ / m²), we refer to Vialle (2011) with a detached house. For the materials cost (MC), pumping system is 2153 (€); secondary filtration is 419 (€); disinfection is 598 (€); the materials cost of tank is 1794 (€) for 5 m². In this study, assuming the material cost of the tank per cubic meter is $1794/5 = 358.8$ (€ / m²). The installation cost(IC) is 4125(€). Power consumption (PC) is 41(€). The materials cost, investment and operating costs associated are presented as:

$$I_{RWH} = V_t \times 358.8 + MC + IC + PC \tag{18}$$

The maintenance and disposal cost of I_{GR} and I_{RWH} overlap, so we included it in I_{GR} . I_{GR} also includes the installation and operation costs. As the observed data in this study is from a semi-intensive GR, we assumed an average of the I_{GR} in France equals averages from references of semi-intensive GR. As reported in Manso et al. (2021), for semi-intensive GR, the average materials and installation cost (MI) is 130 € / m²; the operation and average maintenance cost (OM) is 7.77 € / m² /year; the average disposal cost (DC) is 12 € / m²; and current GR systems are expected to have an average in-service life of 40 years. As in Okoye et al. (2015), the annual discount rate is taken as 6% (i.e., $i = 0.005$ per month). The lifetime of the rainwater tank is assumed to be 25 years. So, in this case the I_{GR} (€ / m²) is:

$$I_{GR} = R_{GR} \times RA \times (MI + DC) + R_{GR} \times RA \times OM \times 40 \tag{19}$$

After generating the Pareto graph, the Compromise Programming (CP) method was employed to identify the optimal solution from the final Pareto set generated by the NSGA-II algorithm. The CP method, a well-established Multiple Criteria Decision Making (MCDM) approach introduced by Hendriks et al. (1992), aims to find a subset of efficient solutions, known as a compromise set, that is closest to the ideal point where all criteria are optimized (Bayesteh and Azari 2021). The CP method can be mathematically expressed as Eq. (20):

$$\text{Min}Z = \left[\sum_{j=1}^n \left(w_j \times \frac{F_j(x) - F_j(x^{*j})}{F_j(x_{*j}) - F_j(x^{*j})} \right)^p \right]^{1/p}, \text{ s.t. } x \in X \tag{20}$$

where,

- x The vector of decision variables
- X The feasible set
- w_j The positive weight for goal j
- x^{*j} Ideal solution for goal j
- x_{*j} The most inappropriate solution based on the objective function j
- p The topological metric; i.e., a real number between 1 and ∞

In this study, equal weightage was given to the F1 and F2 objective functions, with a weightage of 0.5 assigned to both. To enhance the model's capability in selecting the optimal solution, a value of 2 was assigned to parameter p in Eq. (20) (Goorani and Shabanlou 2021). In cases where the Z values of two optimized Vt results are equivalent, preference was given to the one with a lower Vt value, as it corresponds to a smaller footprint.

2.3 Case Study

The present study applied the NSGA-II model to a dataset of daily rainfall spanning 41 years (1980–2020) from the ORLY station (FRM00007149) in Paris, which was obtained from the Global Historical Climatology Network-Daily (GHCN-Daily), Version 3. Paris has a mild maritime climate with an annual average temperature of 10°C, wherein the average temperature in January is 3°C and the average temperature in July is 18°C. Rainfall occurs year-round, with slightly higher precipitation levels in summer and autumn, and an average annual rainfall of 622 mm. To investigate the annual variability, we analyzed 41 years of rainfall data and identified three distinct climatic scenarios, namely a wet year, an average year, and a dry year. The year with the highest and lowest annual rainfall was considered as the wet and dry years, respectively, while the year with annual rainfall close to the 41-year average was considered as the average year (Hajani and Rahman 2014; Karim et al. 2015; Stec and Zelenáková 2019). The annual rainfall data for the wet year (2001), average year (1995), and dry year (2005) were 867.8 mm, 622.6 mm, and 410.4 mm (See Supplementary material, Fig. S1).

In this study, we aimed to investigate the impact of the influence of R_{GR} on Vt by evaluating five different levels of R_{GR} (0, 25, 50, 75 and 100%). $R_{GR}=0\%$ indicated the presence of a traditional impermeable roof, which is the standard for RWH systems. For hydrological calculations, the RWH and GR-RWH systems were treated identically, except for the runoff method and evapotranspiration. The RCM was utilized to convert precipitation to roof runoff in non-GR areas, with evaporation being disregarded, runoff Coefficient was assumed to be 0.9 (Abdulla 2020; Alim et al. 2020; Maykot and Ghisi 2020).

In order to explore the efficiency of different roof sizes and water demands, we assumed different RA. Each RA will run under a set of different water demand and different R_{GR} . The assumed RA and Vt considered in this study were selected based on those reported in previous RWH research (See Supplementary material, Table S1). Given the limited availability of data on roof area distribution in Paris, we explored a wide range of RA, including 50, 100, 200, 300, 500, 800, 1000, 2000, 3000, 5000, and 10000 m². We also assumed a range of values for Vt, with $V_t \in (1m^3, 400m^3)$, in order to capture a broad range of scenarios.

According to data from France's Water Information Centre (Le Centre d'Information sur l'eau) (l'eau 2015), the average water consumption of a toilet flush is assumed to be 9 L, with an average of four flushes per person per day, resulting in a total of 36 L of

water consumed per person per day. Due to uncertainties in the number of occupants in public buildings and daily traffic, it is impractical to accurately determine the actual water demand. Therefore, this study considers 10 different water demand scenarios (0.1, 0.5, 1.0, 1.5, 2.0, 2.5, 3.0, 3.5, 4.0, 4.5, 5.0 m³/d) to explore the impact of Vd on Vt.

3 Results and Discussion

3.1 Calibration and Validation of Conceptual Interflow Model

The initial values of model parameters, such as field moisture capacity and saturated moisture content, as well as a comprehensive description of the CI-model, can be found in Xie and Liu (2020). The model parameters were adjusted using the trial-and-error method to obtain a reasonable fit with the observed data. The corresponding outcomes are presented in Table S2 (See Supplementary material). The NSE values of the CI-model range from 0.565 to 0.936, and Rv values range from 0.827 to 0.971, indicating that the CI-model is capable of accurately simulating GR discharge during rainfall events.

3.2 Five GR Coverage Scenarios

The variations in optimal Vt, WR and P_{ROI} of different RA at different Vd and GR coverage are shown in Fig. 2 and Table 2. Notably, the maximum Vd that can be accommodated by different RA or R_{GR} is dissimilar (WR less than 0.5 is not included in the analysis as it lacks practical significance). For instance, when RA is 50 m², only Vd of 0.1 m³/d can be supported.

According to Fig. 2 and Table 2, it has been observed that when R_{GR} is held constant, an increase in RA leads to an increase in WR, when both RA and Vd are fixed, an increase in R_{GR} does not have a significant impact on WR. However, when Vd is large, WR tends to slightly decrease with an increase in R_{GR}. For example, when RA=3000m² and Vd >0.35 m³/d, there is a slight decrease in WR as R_{GR} increases. Nevertheless, for RA=3000m², Vd < 0.35 m³/d, the WR remains unchanged for different R_{GR} values. The reason for this lies in the fact that as RA increases, the total amount of rainwater available for the system also increases, resulting in an increase in WR. However, as R_{GR} increases, the retention effect of GR on rainwater becomes more pronounced. Although a high level of WR can be maintained by increasing Vt, the total amount of available rainwater continues to decrease, resulting in a slight decrease in WR.

When R_{GR} is held constant, an increase in RA leads to an increase in P_{ROI}, and when the RA and Vd are maintained at a constant level, an increase in R_{GR} results in a corresponding increase in P_{ROI}. The reason for this is that as RA or R_{GR} increases, the construction cost of GR also increases, while the return on investment is insufficient to offset the expenditure. Therefore, P_{ROI} continues to increase.

According to Table 2 and Fig. 2, when Vd was small, Vt increased with the increase of R_{GR}. When Vd was large, Vt increased first and then decreased with the increase of R_{GR}, generally reaching the peak at R_{GR} = 50 or 75%. For example, when RA ≤ 800m², only when Vd = 0.1 m³/d and 0.5 m³/d, Vt increases continuously with the increase of R_{GR}. However, when RA ≤ 800m², Vd ≥ 1.0m³/d, Vt increases first and then decreases with the increase of R_{GR}. The reason is that the increase in R_{GR} leads to a decrease in available rainwater utilization, which necessitates a larger Vt to retain more water during rainy days. When the Vd is relatively high, the high R_{GR} GR-RWH system fails to meet the high WR

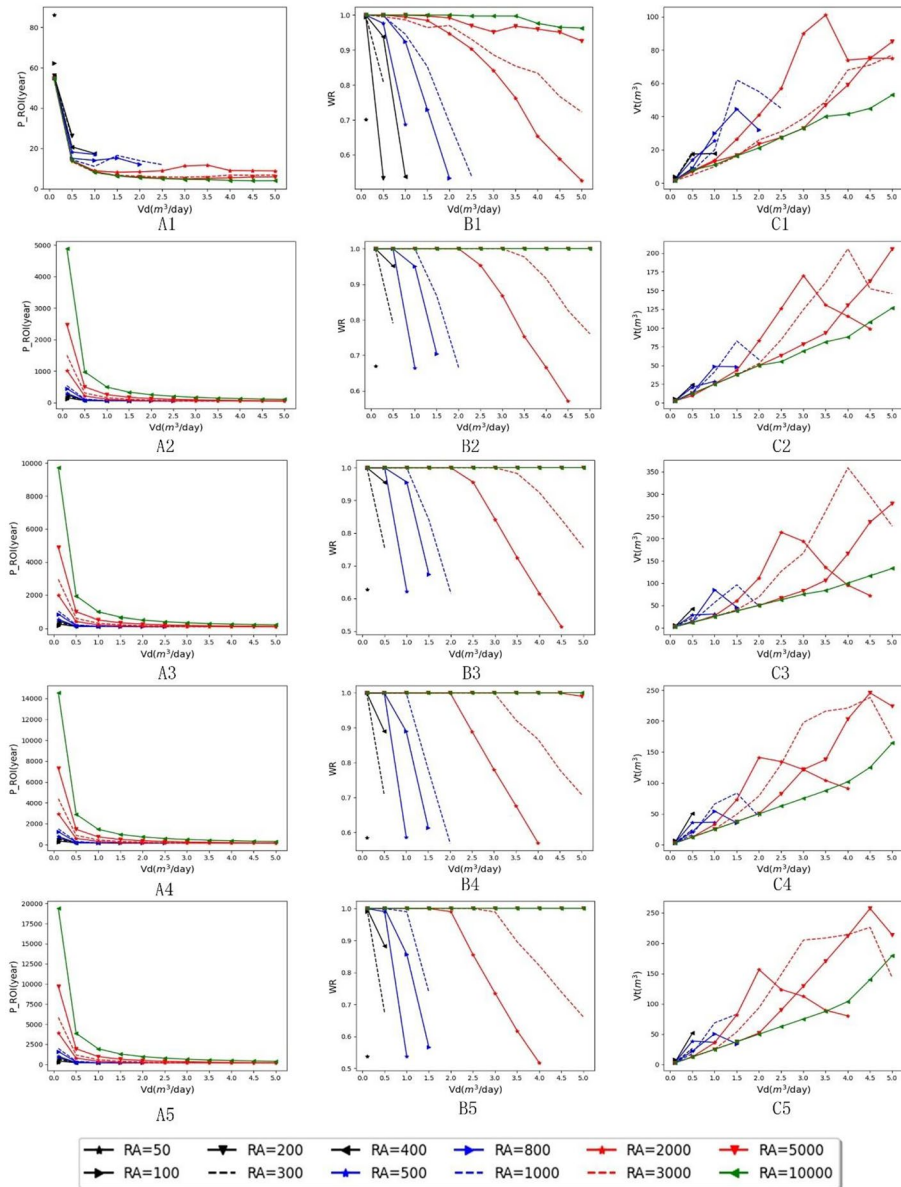


Fig. 2 The V_t , WR and P_{ROI} for different V_d and RA of different GR coverage (A1-A5, were the P_{ROI} for different V_d and RA of different R_{GR} (0, 25, 50, 75, and 100%); B1-B5 were the WR for different V_d and RA of different R_{GR} (0, 25, 50, 75, and 100%); C1-C5 were the V_t for different V_d and RA of different R_{GR} (0, 25, 50, 75, and 100%))

by increasing V_t . Therefore, the NSGA-II optimization objective of P_{ROI} is achieved by slightly reducing V_t .

According to Table 2, for all analyzed scenarios, when $R_{GR} = 0\%$, the optimal V_t is 1.7-101m³ and the maximum WR is 0.52-1.0. The minimum P_{ROI} is 3.9-86.0 years. The

Table 2 Vt, WR and P_{ROI} for different Vd and RA of different R_{GR}

RA(m ²)	Vd(m ³ /d)	R _{GR} =0%			R _{GR} =25%			R _{GR} =50%			R _{GR} =75%			R _{GR} =100%		
		Vt(m ³)	WR	P _{ROI} (year)	Vt(m ³)	WR	P _{ROI} (year)	Vt(m ³)	WR	P _{ROI} (year)	Vt(m ³)	WR	P _{ROI} (year)	Vt(m ³)	WR	P _{ROI} (year)
50	0.1	3.10	0.70	86.09	3.30	0.67	128.60	3.60	0.63	176.57	3.60	0.59	229.41	3.60	0.54	289.11
100	0.1	3.90	0.99	62.17	5.40	1.00	114.04	5.60	1.00	165.88	7.90	1.00	225.36	7.90	0.99	284.83
200	0.1	2.10	1.00	56.23	2.60	1.00	154.14	2.65	1.00	251.98	3.30	1.00	349.94	3.60	1.00	447.82
200	0.5	8.40	0.53	26.37	8.50	0.49	65.54	8.90	0.46	109.25	12.00	0.43	160.41	12.50	0.40	215.73
300	0.1	1.90	1.00	55.57	2.30	1.00	202.02	2.50	1.00	347.75	2.50	1.00	493.37	2.50	1.00	639.01
300	0.5	18.80	0.81	25.25	21.10	0.79	66.43	22.70	0.75	110.53	24.40	0.71	160.60	26.70	0.67	217.20
400	0.1	1.86	1.00	55.30	2.40	1.00	250.51	2.50	1.00	444.55	2.50	1.00	638.62	2.50	1.00	832.74
400	0.5	17.90	0.94	20.75	24.50	0.95	68.10	42.20	0.96	121.52	50.70	0.89	175.22	51.80	0.88	231.90
400	1.0	17.90	0.54	17.47	16.40	0.49	55.52	16.37	0.46	98.43	26.30	0.43	150.39	28.80	0.40	205.51
400	1.5	16.30	0.31	16.37	15.20	0.27	53.73	-	1.00	-	-	1.00	-	-	1.00	-
500	0.1	1.80	1.00	55.15	2.40	1.00	298.86	2.50	1.00	541.25	2.50	1.00	783.72	2.50	0.99	1026.28
500	0.5	14.00	0.98	18.15	21.00	1.00	71.57	28.20	0.62	124.47	35.80	0.59	182.29	38.60	0.54	240.81
500	1.0	25.50	0.69	17.04	28.80	0.66	56.71	-	-	-	-	-	-	-	-	-
800	0.1	1.70	1.00	54.87	2.50	1.00	443.60	2.50	1.00	830.90	2.50	1.00	1218.35	2.50	1.00	1605.96
800	0.5	9.10	1.00	15.07	13.70	1.00	95.39	14.50	1.00	174.28	21.00	1.00	253.60	22.20	1.00	331.91
800	1.0	30.00	0.92	14.03	48.70	0.95	62.40	84.80	0.96	115.98	54.30	0.89	160.35	50.60	0.86	214.91
800	1.5	44.50	0.73	15.23	48.20	0.70	54.63	45.50	0.67	96.88	35.50	0.61	143.54	34.10	0.57	198.01
800	2.0	32.00	0.53	12.03	-	-	-	-	-	-	-	-	-	-	-	-
1000	0.1	1.70	1.00	54.82	2.50	1.00	539.92	2.50	1.00	1023.67	2.50	1.00	1507.66	2.50	1.00	1991.90
1000	0.5	7.50	1.00	14.34	12.60	1.00	113.67	13.20	1.00	211.48	16.40	1.00	309.54	17.90	1.00	407.42
1000	1.0	20.00	0.95	11.06	41.50	1.00	66.27	56.40	1.00	119.29	65.90	1.00	175.50	68.60	0.99	233.08
1000	1.5	62.00	0.85	16.50	82.60	0.87	60.61	96.10	0.84	106.52	83.50	0.78	153.00	82.90	0.74	207.83
1000	2.0	55.00	0.69	13.92	57.70	0.67	52.80	47.60	0.61	94.18	45.40	0.57	142.06	28.30	0.50	197.35
1000	2.5	45.00	0.54	11.92	-	-	-	-	-	-	-	-	-	-	-	-
2000	0.1	1.50	1.00	54.67	2.50	1.00	1021.78	2.50	1.00	1987.23	2.50	1.00	2952.67	2.50	1.00	3919.73
2000	0.5	7.50	1.00	14.01	9.70	1.00	209.83	12.50	1.00	404.21	12.50	1.00	598.27	12.50	1.00	792.39
2000	1.0	13.80	0.99	8.87	25.50	1.00	108.63	26.50	1.00	206.40	32.90	1.00	304.49	35.90	1.00	402.36
2000	1.5	26.50	0.98	8.16	43.50	1.00	76.48	60.50	1.00	143.58	73.00	1.00	209.66	81.90	1.00	276.63
2000	2.0	41.00	0.95	8.38	83.00	1.00	63.65	111.50	1.00	116.53	141.20	1.00	174.07	156.30	0.99	232.90
2000	2.5	57.00	0.90	8.89	126.10	0.95	59.41	214.20	0.96	112.84	134.50	0.89	156.67	123.60	0.86	211.19
2000	3.0	90.00	0.84	11.27	169.90	0.87	58.90	193.80	0.84	104.55	121.50	0.78	147.52	112.30	0.73	200.03
2000	3.5	101.00	0.76	11.70	130.60	0.75	53.40	135.20	0.72	96.26	103.90	0.68	141.62	89.40	0.62	195.27
2000	4.0	74.00	0.65	9.02	115.60	0.67	50.85	95.20	0.61	92.10	90.90	0.57	139.85	80.00	0.52	193.57
2000	4.5	75.00	0.59	8.91	99.00	0.57	49.21	72.00	0.51	90.35	-	-	-	-	-	-
2000	5.0	75.00	0.53	8.81	-	-	-	-	-	-	-	-	-	-	-	-
3000	0.1	1.50	1.00	54.67	2.50	1.00	1504.50	2.50	1.00	2952.67	2.50	1.00	4400.84	2.50	1.00	5849.01
3000	0.5	5.00	1.00	13.32	12.50	1.00	306.83	12.50	1.00	597.54	12.50	1.00	888.37	12.50	1.00	1179.32
3000	1.0	10.00	0.99	8.10	25.00	1.00	156.76	25.00	1.00	302.34	25.00	1.00	447.96	25.00	1.00	593.59
3000	1.5	16.30	0.96	6.61	37.50	1.00	106.92	39.80	1.00	204.71	49.30	1.00	302.80	53.80	1.00	400.68
3000	2.0	26.00	0.97	6.22	52.60	1.00	82.96	68.70	1.00	157.76	78.90	1.00	231.80	93.60	1.00	305.49
3000	2.5	31.00	0.93	5.75	84.50	1.00	70.28	126.50	1.00	131.51	130.50	1.00	191.52	148.50	1.00	229.41
3000	3.0	39.00	0.89	5.76	124.60	1.00	62.78	167.30	1.00	115.67	197.90	1.00	171.98	205.00	0.99	252.42
3000	3.5	49.00	0.85	5.96	160.50	0.98	58.76	261.60	0.98	112.22	216.00	0.92	160.74	208.40	0.90	215.71
3000	4.0	68.00	0.83	6.77	205.70	0.92	58.08	359.00	0.92	111.32	221.00	0.87	152.91	214.00	0.82	207.01
3000	4.5	71.00	0.77	6.68	152.40	0.83	53.29	295.30	0.84	104.16	238.10	0.78	149.08	226.00	0.74	202.88
3000	5.0	71.00	0.72	6.82	145.80	0.76	51.18	227.90	0.76	97.95	171.40	0.71	142.19	142.80	0.66	195.24
5000	0.1	1.70	1.00	54.74	2.50	1.00	2469.95	2.50	1.00	4883.56	2.50	1.00	7297.18	2.50	1.00	9710.80
5000	0.5	7.00	1.00	13.76	12.50	1.00	499.70	12.50	1.00	983.44	12.50	1.00	1467.42	12.50	1.00	1951.65
5000	1.0	13.00	1.00	8.47	25.00	1.00	253.50	25.00	1.00	495.89	25.00	1.00	728.36	25.00	1.00	980.90
5000	1.5	16.80	1.00	6.45	37.50	1.00	171.22	37.50	1.00	332.95	37.50	1.00	494.71	37.50	1.00	656.52
5000	2.0	23.50	0.99	5.74	50.00	1.00	130.02	50.00	1.00	251.37	50.50	1.00	372.87	51.90	1.00	494.37
5000	2.5	27.50	0.97	5.16	63.30	1.00	105.59	66.50	1.00	203.36	82.30	1.00	301.46	89.70	1.00	399.33
5000	3.0	33.00	0.95	4.89	78.40	1.00	89.89	82.90	1.00	171.93	121.80	1.00	254.51	129.20	1.00	336.08
5000	3.5	47.00	0.97	5.16	93.10	1.00	78.54	106.20	1.00	149.47	137.70	1.00	220.60	170.00	1.00	290.98
5000	4.0	59.00	0.96	5.36	130.10	1.00	71.39	166.00	1.00	134.62	203.40	1.00	197.07	212.00	1.00	260.19
5000	4.5	75.00	0.95	5.79	162.30	1.00	66.02	236.90	1.00	123.34	245.50	1.00	179.30	257.00	1.00	339.50
5000	5.0	85.00	0.93	5.88	205.50	1.00	62.02	278.80	1.00	114.97	224.00	0.99	168.11	213.50	1.00	227.51
10000	0.1	1.70	1.00	54.74	2.50	1.00	4883.56	2.50	1.00	9710.80	2.50	1.00	14538.03	2.50	1.00	19365.26
10000	0.5	8.00	1.00	14.11	12.50	1.00	981.62	12.50	1.00	1947.07	12.50	1.00	2912.52	12.50	1.00	3878.56
10000	1.0	11.00	1.00	8.08	25.00	1.00	494.67	25.00	1.00	978.41	25.00	1.00	1462.39	25.00	1.00	1946.62
10000	1.5	16.50	1.00	6.35	37.50	1.00	332.31	37.50	1.00	655.21	37.50	1.00	978.23	37.50	1.00	1301.42
10000	2.0	21.20	1.00	5.42	50.00	1.00	250.98	50.00	1.00	493.37	50.00	1.00	735.84	50.00	1.00	978.38
10000	2.5	27.50	1.00	4.98	55.00	1.00	201.92	62.50	1.00	396.14	62.50	1.00	590.20	62.50	1.00	784.32
10000	3.0	33.00	1.00	4.64	69.00	1.00	169.34	75.00	1.00	331.27	75.00	1.00	493.03	75.00	1.00	654.83
10000	3.5	40.10	1.00	4.51	81.40	1.00	146.03	83.40	1.00	284.90	87.50	1.00	423.58	87.50	1.00	562.30
10000	4.0	41.50	0.98	4.14	88.00	1.00	128.62	100.00	1.00	250.11	101.80	1.00	371.59	103.80	1.00	493.10
10000	4.5	45.00	0.97	3.95	108.00	1.00	115.15	116.40	1.00	223.25	125.10	1.00	331.63	140.00	1.00	440.36
10000	5.0	53.00	0.96	3.98	126.70	1.00	104.58	132.90	1.00	202.35	164.50	1.00	300.45	179.50	1.00	398.32

relevant results of R_{GR}=0% (traditional RWH), are consistent with current similar research (Alim et al. 2020; Maykot and Ghisi 2020; Słyś and Stec 2020; Stec and Zelenáková 2019).

According to Table 2, for all analyzed scenarios, when R_{GR} =25%, the optimal Vt is 2.5-205.7m³ and the maximum WR is 0.57-1.0. The minimum P_{ROI} is 49.2-4883.5 years. When R_{GR} =50%, the optimal Vt is 2.5-359.0m³ and the maximum WR is 0.51-1.0. The minimum P_{ROI} is 89.7-9710.7 years. When R_{GR} =75%, the optimal Vt is 2.5-245.5m³ and the maximum WR is 0.57-1.0. The minimum P_{ROI} is 139.8-14538.0 years. When R_{GR} =100%, the optimal Vt is 2.5-257m³ and the maximum WR is 0.51-1.0. The minimum P_{ROI} is 193.5-19365.3 years. Comparing the results of the 50% and 100% GR coverage scenarios with previous studies, we found that our results were similar to those of Chao-Hsien et al. (2015) and C. Santos and Taveira-Pinto (2013) in terms of water reliability of GR-RWH. However, our economic viability results differed from theirs, with our P_{ROI}

longer. One possible explanation for this disparity is that previous studies only considered the capital costs of RWH, while treating GR as a pre-existing building component. In contrast, our study viewed GR and RWH as an integrated system, assuming that both were installed simultaneously on the building. This approach resulted in a higher total capital cost for the GR-RWH system, which in turn led to longer P_{ROI} .

It also should be noted that this study only focuses on the benefits of GR-RWH for rainwater recycling. Other benefits of GR, such as mitigating the Urban Heat Island Effect (UHIE) (Leal Filho et al. 2017; Susca et al. 2011), stormwater management, urban noise attenuation and air quality improvement (Berardi et al. 2014; Scolaro and Ghisi 2022; Vijayaraghavan 2016) have not been quantified in terms of monetary value. Further research should explore the monetization of various benefits of GR and integrate them into a comprehensive assessment.

4 Conclusions

In this study, we investigated the potential of GR-RWH systems to improve water balance and economic feasibility. Specifically, we applied the NSGA-II algorithm to the CI-WB-model to determine the optimal sizing of a rainwater storage tank for GR-RWH systems in the city of Paris, considering various levels of RA, Vd and R_{GR} . The key findings were:

- (i) Although the GR-RWH requires a larger V_t , it can still achieve a WR comparable to traditional RWH ($RGR = 0\%$).
- (ii) In Paris, GR-RWH systems are viable for multiple R_{GR} , ranging from 25 to 75% for new building designs as rainwater utilization needs are fulfilled at a low cost while also providing additional benefits of GRs. However, this paper does not determine the optimal GR coverage due to the lack of methods for calculating energy and ecological benefits. Inclusion of the economic value of all GR benefits in the analysis would yield a larger range of feasible GR-RWH scenarios.
- (iii) The addition of RWH may bring economic benefits to buildings in Paris that already have a GR.

Supplementary Information The online version contains supplementary material available at <https://doi.org/10.1007/s11269-023-03568-z>.

Authors Contributions Haowen Xie: Data curation, Software, Writing- Original draft preparation. Mark Randal: Writing- Reviewing and Editing. Sylvania Melo dos Santos: Reviewing and Editing.

Availability of Data and Material Not applicable.

Declarations

Ethics Approval Not applicable.

Consent to Participate Not applicable.

Consent to Publish Not applicable.

Competing Interests We declare that we have no financial and personal relationships with other people or organizations that can inappropriately influence our work, there is no professional or other personal interest of any nature or kind in any product, service and/or company that could be construed as influencing the position presented in, or the review of, the manuscript entitled.

References

- Abdulla F (2020) Rainwater harvesting in Jordan: potential water saving, optimal tank sizing and economic analysis. *Urban Water J* 17(5):446–456. <https://doi.org/10.1080/1573062x.2019.1648530>
- Alim MA, Rahman A, Tao Z, Samali B, Khan MM, Shirin S (2020) Feasibility analysis of a small-scale rainwater harvesting system for drinking water production at Werrington, New South Wales, Australia. *J Clean Prod*. 270. <https://doi.org/10.1016/j.jclepro.2020.122437>
- Almeida AP, Liberalesso T, Silva CM, Sousa V (2021) Dynamic modelling of rainwater harvesting with green roofs in university buildings. *J Clean Prod* 312:1. <https://doi.org/10.1016/j.jclepro.2021.127655>
- An KJ, Lam YF, Hao S, Morakinyo TE, Furumai H (2015) Multi-purpose rainwater harvesting for water resource recovery and the cooling effect. *Water Res* 86:116–121. <https://doi.org/10.1016/j.watres.2015.07.040>
- Bayesteh M, Azari A (2021) Stochastic optimization of reservoir operation by applying hedging rules. *J Water Resour Plan Manag* 147(2):04020099. [https://doi.org/10.1061/\(ASCE\)WR.1943-5452.0001312](https://doi.org/10.1061/(ASCE)WR.1943-5452.0001312)
- Berardi U, GhaffarianHoseini A, GhaffarianHoseini A (2014) State-of-the-art analysis of the environmental benefits of green roofs. *Appl Energy* 115:411–428. <https://doi.org/10.1016/j.apenergy.2013.10.047>
- Campisano A, Butler D, Ward S, Burns MJ, Friedler E, DeBusk K, ... Han M (2017) Urban rainwater harvesting systems: Research, implementation and future perspectives. *Water Res* 115:195–209. <https://doi.org/10.1016/j.watres.2017.02.056>
- Carbone M, Garofalo G, Nigro G, Piro P (2014) A conceptual model for predicting hydraulic behaviour of a green roof. *Procedia Eng* 70:266–274. <https://doi.org/10.1016/j.proeng.2014.02.030>
- Cascone S, Coma J, Gagliano A, Perez G (2019) The evapotranspiration process in green roofs: A review. *Build Environ* 147:337–355. <https://doi.org/10.1016/j.buildenv.2018.10.024>
- Chao-Hsien L, En-Hao H, Yie-Ru C (2015) Designing a rainwater harvesting system for urban green roof irrigation. *Water Sci Technol-Water Supply* 15(2):271–277. <https://doi.org/10.2166/ws.2014.107>
- Cirkel DG, Voortman BR, van Veen T, Bartholomeus RP (2018) Evaporation from (blue-)green roofs: Assessing the benefits of a storage and capillary irrigation system based on measurements and modeling. *Water* 10(9). <https://doi.org/10.3390/w10091253>
- Cook LM, Larsen TA (2021) Towards a performance-based approach for multifunctional green roofs: An interdisciplinary review. *Build Environ* 188. <https://doi.org/10.1016/j.buildenv.2020.107489>
- Dallman S, Chaudhry AM, Muleta MK, Lee J (2017) Erratum to: The value of rain: Benefit-cost analysis of rainwater harvesting systems. *Water Resour Manag* 31(13):4373–4374. <https://doi.org/10.1007/s11269-017-1798-z>
- Deb K, Pratap A, Agarwal S, Meyarivan T (2002) A fast and elitist multiobjective genetic algorithm: NSGA-II. *IEEE Trans Evol Comput* 6(2):182–197. <https://doi.org/10.1109/4235.996017>
- Dixon A, Butler D, Fewkes A (1999) Water saving potential of domestic water reuse systems using grey-water and rainwater in combination. *Water Sci Technol* 39(5):25–32. [https://doi.org/10.1016/S0273-1223\(99\)00083-9](https://doi.org/10.1016/S0273-1223(99)00083-9)
- Fewkes A (2000) Modelling the performance of rainwater collection systems: towards a generalised approach. *Urban Water* 1(4):323–333. [https://doi.org/10.1016/S1462-0758\(00\)00026-1](https://doi.org/10.1016/S1462-0758(00)00026-1)
- Francis LFM, Jensen MB (2017) Benefits of green roofs: A systematic review of the evidence for three ecosystem services. *Urban For Urban Green* 28:167–176. <https://doi.org/10.1016/j.ufug.2017.10.015>
- Goorani Z, Shabanlou S (2021) Multi-objective optimization of quantitative-qualitative operation of water resources systems with approach of supplying environmental demands of Shadegan Wetland. *J Environ Manag* 292:112769. <https://doi.org/10.1016/j.jenvman.2021.112769>
- Hajani E, Rahman A (2014) Reliability and cost analysis of a rainwater harvesting system in peri-urban regions of greater Sydney. *Australia Water* 6(4):945–960. <https://doi.org/10.3390/w6040945>
- Hardin M, Wanielista M, Chopra M (2012) A mass balance model for designing green roof systems that incorporate a cistern for re-use. *Water* 4(4). <https://doi.org/10.3390/w4040914>
- Hendriks MMWB, de Boer JH, Smilde AK, Doornbos DA (1992) Multicriteria decision making. *Chemom Intell Lab Syst* 16(3):175–191. [https://doi.org/10.1016/0169-7439\(92\)80036-4](https://doi.org/10.1016/0169-7439(92)80036-4)
- Imteaz MA, Adeboye OB, Rayburg S, Shanableh A (2012) Rainwater harvesting potential for south-west Nigeria using daily water balance model. *Resour Conserv Recycl* 62:51–55. <https://doi.org/10.1016/j.resconrec.2012.02.007>
- Jahanfar A, Drake J, Sleep B, Gharabaghi B (2018) A modified FAO evapotranspiration model for refined water budget analysis for Green Roof systems. *Ecol Eng* 119:45–53. <https://doi.org/10.1016/j.ecoleng.2018.04.021>
- Karim MR, Bashar MZI, Imteaz MA (2015) Reliability and economic analysis of urban rainwater harvesting in a megacity in Bangladesh. *Resour Conserv Recycl* 104:61–67. <https://doi.org/10.1016/j.resconrec.2015.09.010>


- Kolokotsa D, Santamouris M, Zerefos SC (2013) Green and cool roofs' urban heat island mitigation potential in European climates for office buildings under free floating conditions. *Sol Energy* 95:118–130. <https://doi.org/10.1016/j.solener.2013.06.001>
- l'eau CDIS (2015) Le prix du service de l'eau - Cieau | Centre d'information sur l'eau. <https://www.cieau.com/le-metier-de-leau/prix-des-services-deau/>. Accessed Apr 2022
- Leal Filho W, Echevarria L, Omeche V, Al-Amin A (2017) An evidence-based review of impacts, strategies and tools to mitigate urban heat islands. *Int J Environ Res Public Health* 14:1600. <https://doi.org/10.3390/ijerph14121600>
- Lepp NW (2008) Planting green roofs and living walls. *J Environ Qual* 37(6):2408–2408. <https://doi.org/10.2134/jeq2008.0016br>
- Li Y, Babcock RW Jr (2014) Green roof hydrologic performance and modeling: a review. *Water Sci Technol* 69(4):727–738. <https://doi.org/10.2166/wst.2013.770>
- Lynch DF, Dietsch DK (2010) Water efficiency measures at Emory University. *J Green Build* 5(2):41–54. <https://doi.org/10.3390/jgb.5.2.41>
- Manso M, Teotonio I, Silva CM, Cruz CO (2021) Green roof and green wall benefits and costs: A review of the quantitative evidence. *Renew Sustain Energy Rev* 135. <https://doi.org/10.1016/j.rser.2020.110111>
- Maykot JK, Ghisi E (2020) Assessment of a rainwater harvesting system in a multi-storey residential building in Brazil. *Water* 12(2). <https://doi.org/10.3390/w12020546>
- Melville-Shreeve P, Ward S, Butler D (2016) Rainwater harvesting typologies for uk houses: A multi criteria analysis of system configurations. *Water* 8(4). <https://doi.org/10.3390/w8040129>
- Mitchell VG, Cleugh HA, Grimmond CSB, Xu J (2008) Linking urban water balance and energy balance models to analyse urban design options. *Hydrol Process* 22(16):2891–2900. <https://doi.org/10.1002/hyp.6868>
- Monteiro CM, Calheiros CSC, Pimentel-Rodrigues C, Silva-Afonso A, Castro PML (2016) Contributions to the design of rainwater harvesting systems in buildings with green roofs in a Mediterranean climate. *Water Sci Technol* 73(8):1842–1847. <https://doi.org/10.2166/wst.2016.034>
- Nash JE, Sutcliffe IV (1970) River flow forecasting through conceptual models. *J Hydrol*
- Oberascher M, Zischg J, Palermo SA, Kinzel C, Rauch W, Sitzenfrei R (2019) Smart rain barrels: Advanced LID management through measurement and control. Paper presented at the New Trends in Urban Drainage Modelling, Cham
- Oberndorfer E, Lundholm J, Bass B, Coffman RR, Doshi H, Dunnett N, ... Rowe B (2007) Green roofs as urban ecosystems: Ecological structures, functions, and services. *Bioscience* 57(10):823–833. <https://doi.org/10.1641/b5711005>
- Okoye CO, Solyali O, Akintug B (2015) Optimal sizing of storage tanks in domestic rainwater harvesting systems: A linear programming approach. *Resour Conserv Recycl* 104:131–140. <https://doi.org/10.1016/j.resconrec.2015.08.015>
- Palermo SA, Talarico VC, Pirouz B (2019) Optimizing rainwater harvesting systems for non-potable water uses and surface runoff mitigation. Paper presented at the International Conference on Numerical Computations: Theory and Algorithms
- Quaranta E, Dorati C, Pistocchi A (2021) Water, energy and climate benefits of urban greening throughout Europe under different climatic scenarios. *Sci Rep* 11(1):12163. <https://doi.org/10.1038/s41598-021-88141-7>
- Razzaghamanesh M, Beecham S, Kazemi F (2014) Impact of green roofs on stormwater quality in a South Australian urban environment. *Sci Total Environ* 470:651–659. <https://doi.org/10.1016/j.scitotenv.2013.10.047>
- Sadeghi KM, Kharaghani S, Tam W, Gaerlan N, Loáiciga H (2019) Green stormwater infrastructure (GSI) for stormwater management in the City of Los Angeles: Avalon green alleys network. *Environ Process* 6(1):265–281. <https://doi.org/10.1007/s40710-019-00364-z>
- Sampson DA, Cook EM, Davidson MJ, Grimm NB, Iwaniec DM (2020) Simulating alternative sustainable water futures. *Sustain Sci* 15(4):1199–1210. <https://doi.org/10.1007/s11625-020-00820-y>
- Santos C, Taveira-Pinto F (2013) Analysis of different criteria to size rainwater storage tanks using detailed methods. *Resour Conserv Recycl* 71:1–6. <https://doi.org/10.1016/j.resconrec.2012.11.004>
- Santos SM, Ferreira Silva JF, Santos GC, Macedo PMT, Gavazza S (2019) Integrating conventional and green roofs for mitigating thermal discomfort and water scarcity in urban areas. *J Clean Prod* 219:639–648. <https://doi.org/10.1016/j.jclepro.2019.01.068>
- Scolaro TP, Ghisi E (2022) Life cycle assessment of green roofs: A literature review of layers materials and purposes. *Sci Total Environ* 829. <https://doi.org/10.1016/j.scitotenv.2022.154650>
- Singh A, Sarma AK, Hack J (2020) Cost-effective optimization of nature-based solutions for reducing urban floods considering limited space availability. *Environ Process* 7(1):297–319. <https://doi.org/10.1007/s40710-019-00420-8>

- Słyś D (2009) Potential of rainwater utilization in residential housing in Poland. *Water Environ J* 23(4):318–325. <https://doi.org/10.1111/j.1747-6593.2008.00159.x>
- Słyś D, Stec A (2020) Centralized or decentralized rainwater harvesting systems: A case study. *Resources* 9(1). <https://doi.org/10.3390/resources9010005>
- Souto SL, Reis RPA, Campos MAS (2023) Impact of installing rainwater harvesting system on urban water management. *Water Resour Manag* 37(2):583–600. <https://doi.org/10.1007/s11269-022-03374-z>
- Stec A, Zeleňáková M (2019) An analysis of the effectiveness of two rainwater harvesting systems located in central eastern Europe. *Water* 11(3). <https://doi.org/10.3390/w11030458>
- Susca T, Gaffin SR, Dell’Osso GR (2011) Positive effects of vegetation: Urban heat island and green roofs. *Environ Pollut* 159(8–9):2119–2126. <https://doi.org/10.1016/j.envpol.2011.03.007>
- Tamane S, Dey N, Hassanién AE (2021) Security and privacy applications for smart city development. Springer International Publishing Cham
- UN (2015) The Global Goals. from <http://www.globalgoals.org/>
- Van Mechelen C, Dutoit T, Hermy M (2015) Adapting green roof irrigation practices for a sustainable future: A review. *Sustain Cities Soc* 19:74–90. <https://doi.org/10.1016/j.scs.2015.07.007>
- Versini P-A, Stanic F, Gires A, Schertzer D, Tchiguirinskaia I (2020) Measurements of the water balance components of a large green roof in the greater Paris area. *Earth System Science Data* 12(2):1025–1035. <https://doi.org/10.5194/essd-12-1025-2020>
- Vialle C (2011) Etude du comportement hydraulique, physico-chimique et microbiologique d’un système de récupération d’eaux de toiture. Evaluation de l’empreinte environnementale. (PhD Thesis). Retrieved from <https://oatao.univ-toulouse.fr/6935/>
- Vieira N, Queiroz T, Fagundes M, Dallacort R (2013) Potential of utilization of rain water excess for irrigation of green roofs in Mato Grosso, Brasil. *Eng Agric* 33:857–864. <https://doi.org/10.1590/S0100-69162013000400024>
- Vijayaraghavan K (2016) Green roofs: A critical review on the role of components, benefits, limitations and trends. *Renew Sustain Energy Rev* 57:740–752. <https://doi.org/10.1016/j.rser.2015.12.119>
- Xie H, Liu J (2020) A modeling study of the interflow in the green roof. *Urban For Urban Green* 54. <https://doi.org/10.1016/j.ufug.2020.126760>
- Yang S, Ruangpan L, Torres AS, Vojinovic Z (2023) Multi-objective optimisation framework for assessment of trade-offs between benefits and co-benefits of nature-based solutions. *Water Resour Manag* 37(6):2325–2345. <https://doi.org/10.1007/s11269-023-03470-8>
- Zaremba GJ, Traver RG, Wadzuk BM (2016) Impact of drainage on green roof evapotranspiration. *J Irrig Drain Eng* 142(7):04016022. [https://doi.org/10.1061/\(asce\)ir.1943-4774.0001022](https://doi.org/10.1061/(asce)ir.1943-4774.0001022)

Publisher’s Note Springer Nature remains neutral with regard to jurisdictional claims in published maps and institutional affiliations.

Springer Nature or its licensor (e.g. a society or other partner) holds exclusive rights to this article under a publishing agreement with the author(s) or other rightsholder(s); author self-archiving of the accepted manuscript version of this article is solely governed by the terms of such publishing agreement and applicable law.

Authors and Affiliations

Haowen Xie¹  · Mark Randall² · Sylvana Melo dos Santos³

✉ Haowen Xie
xiehaow@zjweu.edu.cn

¹ College of Civil Engineering and Architecture, Zhejiang University of Water Resources and Electric Power, Hangzhou 310018, China

² Department of Geosciences and Natural Resources Management, University of Copenhagen, Frederiksberg, Denmark

³ Department of Civil and Environmental Engineering, Federal University of Pernambuco, Recife, PE, Brazil